Mechanical Signatures of the Current Blockade Instability in Suspended Carbon Nanotubes

G. Micchi, R. Avriller, F. Pistolesi

Signatures of the Current Blockade Instability in Suspended Carbon Nanotubes

G. Micchi,[1] R. Avriller,[1] and F. Pistolesi[1]

[1] *Univ. Bordeaux, LOMA, UMR 5798, Talence, France.*
CNRS, LOMA, UMR 5798, F-33400 Talence, France.

(Dated: July 17, 2015)

Transport measurements allow sensitive detection of nanomechanical motion of suspended carbon nanotubes. It has been predicted that when the electro-mechanical coupling is sufficiently large a bistability with a current blockade appears. Unambiguous observation of this transition by current measurements may be difficult. Instead, we investigate the mechanical response of the system, namely the displacement spectral function; the linear response to a driving; and the ring-down behavior. We find that by increasing the electro-mechanical coupling the peak in the spectral function broadens and shifts at low frequencies while the oscillator dephasing time shortens. These effects are maximum at the transition where non-linearities dominate the dynamics. These strong signatures open the way to detect the blockade transition in devices currently studied by several groups.

PACS numbers: 73.23.Hk, 73.63-b, 85.85.+j

Recently enormous progress has been achieved in the detection of carbon nanotubes (CNT) bending modes by electronic transport measurements [1–13]. Since nanotube oscillators have remarkable mechanical properties, devices with record mass [7] and force [10] sensitivity have been realized. Transport experiments allow information to be obtained on the mechanical mode by measuring different quantities. The main ones are the oscillation amplitude in response to an external drive [1], the oscillator displacement spectral density, $S_{xx}(\omega)$ [10], and, more recently, the ring-down time of the oscillator [13].

The recent experimental advances allow one to view the behavior of such systems in the strong coupling limit from a new perspective. Defining F_0 as the difference of electrostatic force acting on the nanotube when one electron is added to the suspended part and k as the spring constant for its displacement, one can introduce a polaronic energy scale $\varepsilon_P = F_0^2/k$. For a classical system resonating at pulsation ω_0 (much smaller than the bias voltage eV or the temperature T) it has been predicted [14–17] that, if $\varepsilon_P \gg eV$ and T, the current in the device can be blocked and a bistability can appear (e is the electron charge and we set both the Planck and Boltzmann constant to 1). The energy ε_P can be estimated for actual experiments: For a CNT of 1 μm length, 1 nm radius, and suspended at a distance $d = 500$ nm from a gate one finds $\omega_0/2\pi \approx 50$ MHz, $F_0 = 10^{-14}$ N, $k = 4 \cdot 10^{-4}$ N/m, and thus $\varepsilon_P \approx 16$ mK. One should thus work at very low temperatures $\ll 16$ mK: This is probably why the current blockade transition has not yet been observed for mechanical bending modes. While a (Franck-Condon) blockade [18, 19] has been observed [20] for breathing modes in the regime of incoherent transport. To increase ε_P one can reduce the distance of the CNT from the gate electrode or operate the system close to the Euler buckling instability [21, 22]. The energy ε_P scales quadratically with d, it is thus realistic to increase this energy up to the Kelvin range by reducing the distance d to 100 nm. In any case, a clear observation of the transition will require temperatures of the order 100 mK. At such low temperatures the typical tunnelling rate Γ becomes larger than T, leading to coherent transport through the CNT. In this regime the current blockade can take place only if ε_P is larger than a critical value ε_c of the order of Γ [14, 15]. Since one of the main experimental difficulties is to reach large values of ε_P, the case $\varepsilon_P \sim \Gamma$ is particularly interesting. The transition could then be investigated at fixed and low V and T by varying ε_P, that can be tuned with the gate voltage. One drawback of this limit is the large width Γ of the electronic level: The conductance dependence on ε_P is smooth on the scale Γ failing to provide a clear indication of the transition.

In this Letter we show that, similar to critical phenomena, the transition can be better investigated by looking at the behavior of the phonon mode that becomes soft for $\varepsilon_P = \varepsilon_c$. We study $S_{xx}(\omega)$, the driving response function, and the dephasing and ring-down time as a function of the coupling constant ε_P. We find that all of these quantities have a very peculiar behavior at the transition. The dynamics of the mechanical mode is dominated by nonlinear terms leading to a separation of time scales that is maximal at the transition. The theory presented gives clear indication on how to unambiguously observe the transition using available methods of measurement.

The model. We consider a suspended CNT. We assume that a single electronic level is relevant for transport. We neglect the spin degrees of freedom. The Hamiltonian reads:

$$H = H_L + H_R + H_T + (\epsilon_0 - xF_0)d^\dagger d \ + \frac{p^2}{2m} + \frac{k}{2}x^2 \,, \quad (1)$$

where d is the destruction operator for the electronic level on the dot, x is the displacement of the relevant mechanical mode, p the conjugated momentum, m the mode effective mass, k the spring constant (giving a pulsation $\omega_0 = \sqrt{k/m}$) and F_0 the electrostatic force acting on the dot when an electron is added. The first three terms describe the leads and their coupling:

$H_\alpha = \sum_k (\epsilon_{\alpha k} - \mu_\alpha) c^\dagger_{\alpha k} c_{\alpha k}$, with $\alpha = L$ and R, for left and right lead, $\epsilon_{\alpha k}$ the electronic spectrum, μ_α the chemical potential; and $H_T = \sum_k t_\alpha c^\dagger_{\alpha k} d$ +h.c. the tunnelling Hamiltonian. From these quantities one can define the single-level width $\Gamma_\alpha \equiv \pi t_\alpha^2 \rho_\alpha$ with ρ_α the density of states and $\Gamma = \Gamma_L + \Gamma_R$.

In the Born-Oppenheimer limit ($\Gamma_\alpha \gg \omega_0$) the displacement of the mechanical mode can be described by a Langevin equation:

$$m\ddot{x} + A(x)\dot{x} + m\omega_0^2 x = F_e(x) + \xi(t)\,, \qquad (2)$$

where the dissipation $A(x)$, the average force $F_e(x) = F_0\langle d^\dagger d\rangle$, and the stochastic force $\xi(t)$ are due to the electrons tunneling through the quantum dot [15, 16]. The explicit expressions for A, F_e, and $\langle \xi(t)\xi(t')\rangle = D(x)\delta(t-t')$ have been obtained in Ref. [15]:

$$F_e(x) = F_0\left[\frac{1}{2} + \frac{1}{\pi}\sum_\alpha \frac{\Gamma_\alpha}{\Gamma}\arctan\frac{\mu_\alpha - \epsilon_0 - F_0 x}{\Gamma}\right], \quad (3)$$

$A(x) = (F_0^2\Gamma/\pi)\sum_\alpha \Gamma_\alpha/[(\mu_\alpha - \epsilon_0 - F_0 x)^2 + \Gamma^2]^2$, and $D(x) = F_0^2\Gamma_L\Gamma_R/(\pi\Gamma^3)[h(\mu_L) - h(\mu_R)]$, where $h(\mu) = \arctan z + z/(z^2+1)$ with $z = (\mu - \epsilon_0 - F_0 x)/\Gamma$. In the same limit a Fokker-Planck equation for the probability $P(x,p,t)$ can be derived [23, 24]:

$$\partial_t P = \frac{p}{m}\partial_x P - F\partial_p P + \frac{A}{m}\partial_p(pP) + \frac{D}{2}\partial_p^2 P\,, \qquad (4)$$

with $F(x) = F_e(x) - kx$.

Softening of the mechanical mode. We assume that the device is symmetric: $\Gamma_\alpha = \Gamma/2$. The presence of the mechanical coupling modifies the electron-hole symmetry point for ϵ_0 to the value $\epsilon_0 = (\mu_L + \mu_R)/2 + \varepsilon_P/2$. We will always assume this value from this point on. Defining $y = x - F_0/2k$, one determines $F(y) = -ky + (F_0/2\pi)\sum_{a=\pm1}\arctan[(F_0 y + aeV/2)/\Gamma]$ which depends only on the bias voltage $eV = \mu_L - \mu_R$ and is antisymmetric in y. The equilibrium positions are defined by the solutions of the equation $F(y) = 0$. The line $\varepsilon_P = \varepsilon_c(V) \equiv \pi\Gamma[1 + (eV/2\Gamma)^2]$ [for $eV/\Gamma < 2/\sqrt{3}$] separates the monostable region from the bistable region (see inset of Fig. (1)).

Let us now define ω_m at a stable point y_β as $m\omega_m^2 = -(dF/dy)_{y_\beta}$. It goes smoothly from ω_0 to 0 for $\varepsilon_P < \varepsilon_c$ with the analytic form $\omega_m^2/\omega_0^2 = (\varepsilon_c - \varepsilon_P)/\varepsilon_c$, while for $\varepsilon_P \gtrsim \varepsilon_c$ it reads $2(\varepsilon_P - \varepsilon_c)/\varepsilon_c$ [see Fig. (1) orange dashed lines].

The vanishing of ω_m suggests that its direct measurement should allow the detection of the transition with great accuracy. As in phase transitions, this mode becomes soft, leading to a strong response at the transition. The dip in the gate voltage dependence of ω_m observed by four different groups [3, 4, 9, 12] is the precursor of this softening. Nevertheless, one should be cautious since the definition of ω_m only takes into account the first derivative of the force at the minimum of the potential. When this term vanishes the next order terms in y become important and the response of the system can no longer be predicted simply by the value of ω_m. Therefore, in the following we calculate the typical measurable quantities and study their behavior when ε_P is swept through the transition.

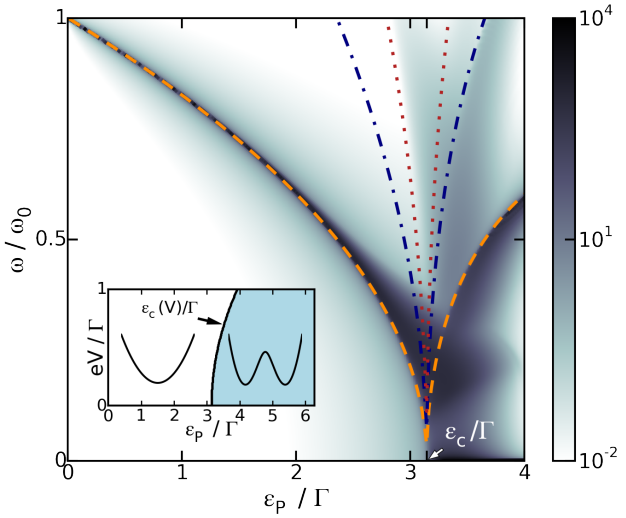

FIG. 1. Density plot of S_{xx} as a function of ω and ε_P. The values of ω_m (orange dashed line), $2\omega_m$ (blue dot-dashed line), and $3\omega_m$ (red dotted line) are shown. The units of S_{xx} are $x_{\rm zpm}^2/\omega_0 = (m\omega_0^2)^{-1}$, where $x_{\rm zpm} = (m\omega_0)^{-1/2}$ is the zero-point motion displacement. The symmetry of the potential implies that only odd harmonics are present for $\varepsilon_P < \varepsilon_c$. Inset: phase diagram in the plane eV-ε_P for the stability of the effective potential.

Fluctuation spectrum. We define the displacement fluctuation spectrum $S_{xx}(\omega) = \int e^{i\omega t} dt \langle \tilde{x}(t)\tilde{x}(0)\rangle$, with $\tilde{x}(t) = x(t) - \langle x\rangle$. This quantity has been measured recently in Ref. [10]. We can obtain S_{xx} numerically from the Fokker-Planck description following the method used in Ref. [17]. Writing Eq. (4) as $\partial_t P = \mathcal{L}_0 P$ the spectrum takes the form:

$$S_{xx}(\omega) = -2{\rm Tr}\left[\hat{\tilde{x}}\frac{\mathcal{L}_0}{\omega^2 + \mathcal{L}_0^2}\hat{\tilde{x}}P_{\rm st}\right] \qquad (5)$$

where $P_{\rm st}$ is the stationary solution of the problem, satisfying both $\mathcal{L}_0 P_{\rm st} = 0$ and the normalization condition ${\rm Tr}P_{\rm st} = 1$. The operator $\hat{\tilde{x}}$ is defined as $\hat{\tilde{x}}P \equiv \tilde{x}P(x,p)$.

Let's begin by discussing the stationary solution of Eq. (4): $P_{\rm st}$. In agreement with similar models [22, 25] we find that for sufficiently small eV, even if the system is out of equilibrium, the stationary distribution function takes the simple Gibbs form $P_{\rm st}(x,p) = \mathcal{N}\exp\{-E(x,p)/T_{\rm eff}\}$, with $T_{\rm eff} = eV/4$, $\mathcal{N}$ a normalization factor, $E(x,p) = p^2/2m + U(x)$, $U(x) = -dF/dx$, and $U(x) = 0$ at its minimum. This result is due to the smooth dependence on x of both $D(x)$ and $A(x)$ on the scale of the spread of the probability distribution $P(x,p)$ for $eV \ll \Gamma$.

We come now to the displacement spectrum obtained

from Eq. (5) that we show for $eV/\Gamma = 5 \cdot 10^{-3}$ in Fig. 1 and 2. As anticipated, as coupling increases the resonance broadens and shifts at low frequency. More surprisingly, the peak position shows a minimum at a small but finite value of ω at the transition with a maximal broadening (cf. Fig. 2-b). The position of the minimum and its width depend on the bias voltage. A strong telegraph noise appears for $\varepsilon_P \gtrsim \varepsilon_c$ (dark region at $\omega \to 0$), signaling the hopping of the systems between the two minima in the potential [15, 17]. This is also a strong indication of the transition [see Fig. (2)-d]. In the bistable phase ($\varepsilon_P > \varepsilon_c$) a double peak in the spectral function is visible.

In order to understand this behavior we take advantage of the separation of time scales of the problem. The damping $A(x)$ and the fluctuations $D(x)$ are both generated by the non-equilibrium electronic transport and, by hypothesis, are parametrically smaller (as ω_0/Γ) than the Hamiltonian terms in Eq. (4). This implies that the system performs many oscillations on the closed trajectory in the phase space that satisfies $E(x(t), p(t)) = E$, before drifting to a nearby trajectory on the slow time scale γ_E^{-1}, where $\gamma_E = \int dx P_{\rm st}(x,p) A(x)/m$ is the average dissipation coefficient [16, 23]. For each energy E one can then calculate the pulsation of the closed trajectory $\omega(E) = 1/\left[2\pi(m/2)^{1/2} \oint [E - U(x)]^{-1/2} dx\right]$. The non-linearities present in $U(x)$ induce dispersion in $\omega(E)$. Then, from our definition, ω_m indicates only $\omega(0)$. Energies up to eV are populated as an effect of the stochastic fluctuations. They all contribute to the fluctuation spectrum leading to an inhomogeneous broadening that spans the frequencies between ω_m and $\omega(eV)$.

In order to provide a quantitative verification of this interpretation we calculate the spectrum by neglecting the effect of the dissipation and considering only the interference of the different trajectories populated according to $P_{\rm st}$ [26, 27]. This gives $S_{xx}(t) = \int dx_0 dy_0 P_{\rm st}(x_0, p_0) \tilde{x}(t) \tilde{x}(0)$, where $x(t)$ satisfies the equation of motion $m\ddot{x} = F(x)$, with the initial conditions $x(0) = x_0$, and $\dot{x}(0) = p_0/m$. In terms of the Fourier coefficients of fixed energy periodic trajectories $[\tilde{x}_E(t) = \sum_n e^{in\omega(E)t} x_n(E)]$ the spectrum takes the form:

$$S_{xx}(\omega) = \int_0^\infty \mathcal{P}(E) dE \sum_n 2\pi\delta(\omega - n\omega(E)) x_n^2(E)\,, \quad (6)$$

with $\mathcal{P}(E) = \mathcal{N} e^{-E/T_{\rm eff}} 2\pi/\omega(E)$.

Two limits can be analyzed [28]: When the quartic term is much smaller than the quadratic one, the full width at half height of the resonance is $\Delta\omega \approx 1.5\omega_0 (eV/\varepsilon_c)(\varepsilon_P/\varepsilon_c)^2 (1 - \varepsilon_P/\varepsilon_c)^{-3/2}$ with a small positive shift of the maximum from ω_m of the same order. In the opposite limit of vanishing harmonic term ($\varepsilon_P = \varepsilon_c$) the potential can be approximated as quartic. In this case $\Delta\omega/\omega_0 = 0.50(eV/\Gamma)^{1/4}$ with a peak position ω_M at $0.85\omega_0 (eV/\Gamma)^{1/4}$. This voltage dependence can be related to the dispersion of $\omega(E)$ that vanishes as $E^{1/4}$ for

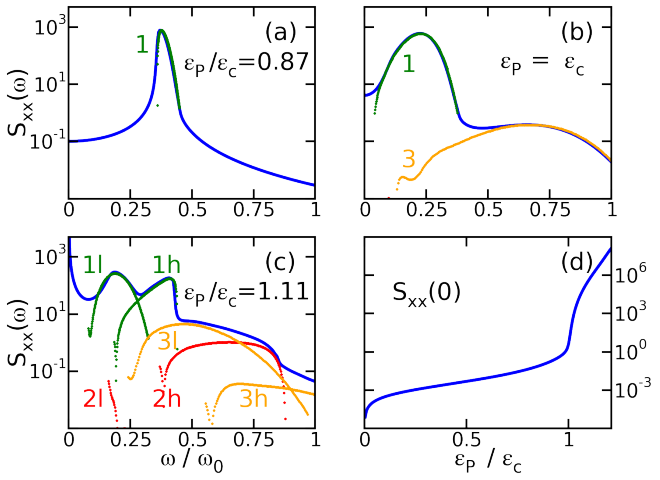

FIG. 2. Comparison of the full numerical solution of the Fokker-Planck equation for S_{xx} (blue solid lines) with the one obtained with Eq. (6) (dots) for $\varepsilon_P/\varepsilon_c = 0.87$, 1, 1.11 (a, b, and c panel, respectively) in units of $(m\omega_0^2)^{-1}$. The numbers label the order of the harmonic, while the letters h and l in the c panel indicate the high- and low-frequency contributions. Panel d: $S_{xx}(0)$ as a function of ε_P/Γ indicating the onset of the telegraph noise at the transition.

$\varepsilon_P = \varepsilon_c$. Remarkably, at criticality the Q-factor of the oscillator defined as $\omega_M/\Delta\omega$ takes the *universal value* 1.71, independently of V or Γ. The crossover between the two regimes takes place for $1 - \varepsilon_P/\varepsilon_c \approx 1.71(eV/\varepsilon_c)^{1/2}$, thus for the values considered in Fig. 1 the quartic region is restricted to $1 - \varepsilon_P/\varepsilon_c < 0.03$. Finally, the double peak of the spectral function for $\varepsilon_P > \varepsilon_c$ can be explained by the contributions of the low-energy high-frequency trajectories around each single minimum, and those, at higher energy and lower frequency, revolving around both minima. The comparison with the numerical result presented in Fig. (2) shows a very good agreement.

Driving. Let us consider the other main tool used to detect mechanical motion: The response to a driving force of frequency ω_D. We can find the linear response of the system by letting $F(x) \to F(x) + F_D \cos(\omega_D t)$ in Eq. (4). The evolution operator becomes $\mathcal{L}(t) = \mathcal{L}_0 + 2\mathcal{L}_D \cos(\omega_D t)$, with $\mathcal{L}_D = -F_D \partial_p/2$. After a transient time the solution can be written as a Fourier series $P(t) = \sum_n e^{in\omega_D t} P_n$ where each Fourier component can in turn be expanded as a power series of the driving parameter F_D: $P_n = \sum_{k=0}^\infty P_{n,k}$, with $P_{n,k}$ of order F_D^k. This leads to the equation for each component $(in\omega_D - \mathcal{L}_0) P_{n,0} = 0$ and

$$(in\omega_D - \mathcal{L}_0) P_{n,k+1} = \mathcal{L}_D (P_{n+1,k} + P_{n-1,k}), \quad (7)$$

with the condition ${\rm Tr} P(t) = 1$. Eq. (7) can be solved by recursion. The time dependence of the displacement then reads $\tilde{x}(t) \equiv {\rm Tr}\left[\hat{\tilde{x}} P(t)\right] = F_D \chi(\omega_D) e^{i\omega_D t} + {\rm c.c.}$, where

$$\chi(\omega) = {\rm Tr}\left[\hat{\tilde{x}} P_1(t)\right] = {\rm Tr}\left[\hat{\tilde{x}} (i\omega - \mathcal{L}_0)^{-1} \partial_p P_{\rm st}\right]\,. \quad (8)$$

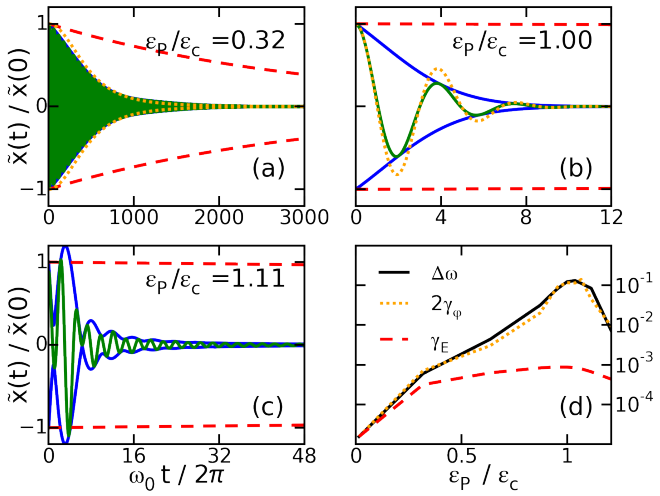

FIG. 3. Time dependence of $\langle\tilde{x}(t)\rangle$ (green solid line) and its envelope (blue solid line) for $\varepsilon_P/\varepsilon_c = 0.32$, 1, and 1.11 (a, b, and c panel, respectively). The exponential decay on the scale $2/\gamma_E$ is shown red dashed. In panel a and b the orange dotted line gives the result of the analytical expressions discussed in the text. Panel d: comparison of the ε_P-dependence of $\Delta\omega$, $2\gamma_\varphi$, and γ_E.

Naturally, the relation between $\chi(\omega)$ and $S_{xx}(\omega)$ comes into question. If $P_{\rm st}$ has a Gibbs form then $F_D\mathcal{L}_0\hat{\tilde{x}}P_{\rm st} = -2T_{\rm eff}\mathcal{L}_D P_{\rm st}$. This leads to a fluctuation-dissipation relation:

$$\mathrm{Im}\left[\chi(\omega)\right] = \frac{\omega}{2T_{eff}} S_{xx}(\omega)\,. \qquad (9)$$

Thus, for $eV \ll \Gamma$, χ and S_{xx} give access to the same information in two independent ways. For larger voltages expression (8) always holds while Eq. (9) will be violated.

Ring-down behavior. Finally, let us consider the response for time $t > 0$ of the oscillator when the coherent drive is switched off at $t = 0$. A damped harmonic oscillator relaxes exponentially on a time scale (the ring-down time) given by the same dissipation coefficient that also determines the width of the resonance of the response function. For nano-mechanical oscillators it has recently been shown [13] that this may not be the case. Nonlinearities induce frequency noise, which in turn is responsible for phase fluctuations of $\tilde{x}(t)$. The average over many realizations of $\tilde{x}(t)$ decays then on the time scale γ_φ^{-1}, the value for which phase fluctuations become the order of 2π. Since the energy is insensitive to the phase, its average decays on the same time scale as the single realization γ_E^{-1}.

With respect to our problem, we use the solution of the Fokker-Planck equation with driving [Eq. (7)] as the initial condition and then find $\tilde{x}(t)$ and $E(t)$ from the evolution of the probability with $\mathcal{L}_0$. The result as a Laplace transform reads:

$$\langle\tilde{x}(z)\rangle = \mathrm{Tr}\left[\hat{\tilde{x}}(z-\mathcal{L}_0)^{-1}P(t=0)\right]\,. \qquad (10)$$

In a similar way we can calculate also the Laplace transform of the evolution of the total energy by letting $\hat{\tilde{x}} \to E(\hat{x},\hat{p})$ in Eq. (10). One can then obtain the time dependence by numerically implementing the Cauchy theorem $\langle\tilde{x}(t)\rangle = \oint_C \langle\tilde{x}(z)\rangle e^{-zt}dz/(2\pi i)$, where C is a contour that encloses the poles of $\langle\tilde{x}(z)\rangle$ for $\mathrm{Re}z < 0$.

We find that the energy exponentially decays on the scale γ_E^{-1}, even at the transition. On the other hand, as shown in Fig. (3), $\langle\tilde{x}(t)\rangle$ decays on a much shorter scale that we define γ_φ^{-1}. Fig. (3)-d shows the ε_P dependence of $\Delta\omega$, $2\gamma_\varphi$, and γ_E. The width $\Delta\omega$, obtained from the form of S_{xx}, coincides within the numerical accuracy with $2\gamma_\varphi$, proving that frequency noise is the responsible of the faster decay of $\langle\tilde{x}(t)\rangle$. Both present a pronounced maximum at $\varepsilon_P = \varepsilon_c$, indicating the transition. Using the approach presented for the analytical calculation of $S_{xx}(\omega)$ we find that $\langle\tilde{x}(t)\rangle$ decays as $1/(1+t^2\gamma_\varphi^2)^2$, where $\gamma_\varphi = 0.41\Delta\omega$ [29]. Similarly for $\varepsilon_P = \varepsilon_c$ the decay scale is proportional to $\Delta\omega$ with the analytical form given by the dotted line of Fig. (3).

Conclusions. We found that the study of the mechanical properties of the suspended carbon nanotube open new perspectives for the observation of the current-blockade transition occurring at low temperaure and voltage for $\varepsilon_P = \pi\Gamma$. Indeed, for that value the quadratic part of the effective potential vanishes, leading to strong frequency and phase fluctuations that remarkably modify the typically measured response functions (S_{xx}, χ, and ring-down behavior). The Q-factor of the resonator takes the minimum and universal value 1.71 at criticality, where the separation of time scales is also maximal. These results can lead to the observation of the current-blockade transition by mechanical measurements in devices currently investigated by several experimental groups.

Acknowledgements. We acknowledge support from ANR-10-BLANC-0404 QNM.

[1] V. Sazonova, Y. Yaish, H. Üstünel, D. Roundy, T. A. Arias, and P. L. McEuen, Nature **431**, 284 (2004).
[2] B. Lassagne, D. Garcia-Sanchez, A. Aguasca, and A. Bachtold, Nano Lett. **8**, 3735 (2008).
[3] G. A. Steele, A. K. Hüttel, B. Witkamp, M. Poot, H. B. Meerwaldt, L. P. Kouwenhoven, and H. S. van der Zant, Science **325**, 1103 (2009).
[4] B. Lassagne, Y. Tarakanov, J. Kinaret, D. Garcia-Sanchez, and A. Bachtold, Science **325**, 1107 (2009).
[5] A. Eichler, J. Moser, J. Chaste, M. Zdrojek, I. Wilson-Rae, and A. Bachtold, Nat Nano **6**, 339 (2011).
[6] E. A. Laird, F. Pei, W. Tang, G. A. Steele, and L. P. Kouwenhoven, Nano letters **12**, 193 (2011).
[7] J. Chaste, A. Eichler, J. Moser, G. Ceballos, R. Rurali,

and A. Bachtold, Nature Nanotechnology **7**, 301 (2012).
[8] H. B. Meerwaldt, G. Labadze, B. H. Schneider, A. Taspinar, Y. M. Blanter, H. S. J. van der Zant, and G. A. Steele, Physical Review B **86** (2012), 10.1103/PhysRevB.86.115454.
[9] M. Ganzhorn and W. Wernsdorfer, Phys. Rev. Lett. **108**, 175502 (2012).
[10] J. Moser, A. Eichler, J. Güttinger, M. I. Dykman, and A. Bachtold, Nat Nano **9**, 1007 (2014).
[11] Y. Zhang, J. Moser, J. Güttinger, A. Bachtold, and M. Dykman, Phys. Rev. Lett. **113**, 255502 (2014).
[12] A. Benyamini, A. Hamo, S. V. Kusminskiy, F. von Oppen, and S. Ilani, Nature Physics **10**, 151 (2014).
[13] B. H. Schneider, V. Singh, W. J. Venstra, H. B. Meerwaldt, and G. A. Steele, Nat Commun **5** (2014), 10.1038/ncomms6819.
[14] M. Galperin, M. A. Ratner, and A. Nitzan, Nano Lett. **5**, 125 (2005).
[15] D. Mozyrsky, M. B. Hastings, and I. Martin, Phys. Rev. B **73**, 035104 (2006).
[16] F. Pistolesi and S. Labarthe, Physical Review B **76** (2007), 10.1103/PhysRevB.76.165317.
[17] F. Pistolesi, Y. Blanter, and I. Martin, Physical Review B **78** (2008), 10.1103/PhysRevB.78.085127.
[18] S. Braig and K. Flensberg, Phys. Rev. B **68**, 205324 (2003).
[19] J. Koch and F. von Oppen, Phys. Rev. Lett. **94**, 206804 (2005).
[20] R. Leturcq, C. Stampfer, K. Inderbitzin, L. Durrer, C. Hierold, E. Mariani, M. G. Schultz, F. von Oppen, and K. Ensslin, Nat Phys **5**, 327 (2009).
[21] G. Weick, F. Pistolesi, E. Mariani, and F. von Oppen, Physical Review B **81** (2010), 10.1103/PhysRevB.81.121409.
[22] G. Weick, F. von Oppen, and F. Pistolesi, Physical Review B **83** (2011), 10.1103/PhysRevB.83.035420.
[23] Y. M. Blanter, O. Usmani, and a. Y. V. Nazarov, Phys. Rev. Lett. **93**, 136802 (2004).
[24] Y. M. Blanter, O. Usmani, and a. Y. V. Nazarov, Phys. Rev. Lett. **94**, 049904 (2005).
[25] A. D. Armour, M. P. Blencowe, and Y. Zhang, Phys. Rev. B **69**, 125313 (2004).
[26] M. I. Dykman and M. A. Krivoglaz, Physica A: Statistical Mechanics and its Applications **104**, 495 (1980).
[27] M. I. Dykman, S. M. Soskin, and M. A. Krivoglaz, Physica A: Statistical Mechanics and its Applications **133**, 53 (1985).
[28] See supplemental materials Sec. I.
[29] See supplemental materials Sec. II.